Transportation-cyber-physical-systems-oriented engine cylinder pressure estimation using high gain observer

Li Yong-Fu, Kou Xiao-Pei, Zheng Tai-Xiong, Li Yin-Guo

What follows is a list of articles you may be interested in

A new collision avoidance model for pedestrian dynamics

Transport path optimization algorithm based on fuzzy integrated weights

Biham-Middleton-Levine model in consideration of cooperative willingness

The effect of moving bottlenecks on a two-lane traffic flow

Investigation of merging and diverging cars on a multi-lane road using cellular automation model

----

Chinese Physics B (First published in 1992)

Transportation-cyber-physical-systems-oriented engine cylinder pressure estimation using high gain observer[*]

Li Yong-Fu(李永福)[†],   Kou Xiao-Pei(寇晓培),   Zheng Tai-Xiong(郑太雄), and Li Yin-Guo(李银国)

Center for Automotive Electronics and Embedded System, College of Automation, Chongqing University of Posts and Telecommunications, Chongqing 400065, China

In transportation cyber-physical-systems (T-CPS), vehicle-to-vehicle (V2V) communications play an important role in the coordination between individual vehicles as well as between vehicles and the roadside infrastructures, and engine cylinder pressure is significant for engine diagnosis on-line and torque control within the information exchange process under V2V communications. However, the parametric uncertainties caused from measurement noise in T-CPS lead to the dynamic performance deterioration of the engine cylinder pressure estimation. Considering the high accuracy requirement under V2V communications, a high gain observer based on the engine dynamic model is designed to improve the accuracy of pressure estimation. Then, the analyses about convergence, converge speed and stability of the corresponding error model are conducted using the Laplace and Lyapunov method. Finally, results from combination of Simulink with GT-Power based numerical experiments and comparisons demonstrate the effectiveness of the proposed approach with respect to robustness and accuracy.

Keywords: transportation cyber-physical-systems, high gain observer, cylinder pressure estimation, vehicle-to-vehicle communications

PACS: 89.40.–a

DOI: 10.1088/1674-1056/24/5/058901

1. Introduction

Transportation cyber-physical systems (T-CPS) are envisioned to achieve full coordination and optimization of transportation systems via the increased interaction and feedback between the transportation cyber systems and transportation physical systems.[1–5] Wherein, vehicle-to-vehicle (V2V) communications play an important role in the coordination between individual vehicles as well as between vehicles and the roadside infrastructures.[6–11] In this context, the V2V-based communication of information on the engine cylinder pressure of the preceding vehicles enables a following vehicle in that platoon to react autonomously to avoid a collision. In addition, information of engine cylinder pressure can be used not only as a feedback signal of closed-loop combustion control for the engine control but also as a cylinder misfire detection signal for engine online fault diagnosis.[12–16] Therefore, accurate estimation of engine cylinder pressure is of importance within the information exchange process under V2V communications.

This study is motivated by the need for a more accurate and robust observer so that the safety of vehicular traffic flow can be improved under a stimulus through V2V communications related to the engine cylinder pressure. To the best of our knowledge, the existing approaches to obtain information about the engine cylinder pressure can be classified roughly

as a direct or an indirect approach. From the direct approach perspective, a variety of high-precision cylinder pressure sensors have been developed. However, the availability of sensors is often limited by their costs, durability, and the installation space in the vehicular engine. Consequently, it is difficult in reality to achieve the control or diagnosis of engine state because of the way that the sensors are installed directly.[16,17] Therefore, the indirect approach, which can obtain an estimation of cylinder pressure via information about the engine, becomes more attractive because of its low cost and simple structure.

In general, the indirect ways to achieve the cylinder pressure estimation can be categorized as: (i) the Kalman-filter, (ii) cepstrum algorithm, and (iii) sliding mode technique. On the Kalman-filter aspect, Durrra *et al.*[18] and Ozawa *et al.*[19] proposed an engine model represented by a time varying linear fist-order differential equation, and the cylinder pressure was reconstructed through a Kalman-filter-based deconvolution algorithm. However, the reconstruction is carried out via the feedforward method, which can deteriorate the accuracy of estimation due to the noise in actual operation. On the cepstrum aspect, Moro *et al.*[20] and Hamedovic *et al.*[21] proposed a cepstrum algorithm to reconstruct the cylinder pressure using the vibration signals of engine. However, it is essentially a kind of off-line algorithm and is not suitable for on-board real-time diagnosis. In addition, the influence of road conditions

http://iopscience.iop.org/cpb   http://cpb.iphy.ac.cn

and the vibration of the engine accessories are significant for the accuracy of pressure estimation. On the sliding mode technique, the sliding mode observer (SMO) for cylinder pressure estimation has received wide attention because of its good performance, such as robustness, convergence and accuracy.[22] For example, Veluvolu et al.[23] and Shiao et al.[24] estimated the cylinder pressure using a sliding observer, which could correct the error automatically based on the engine speed error. However, the performance of the observer mainly depends on the accuracy of the engine model, which can be affected by parametric uncertainties, such as efficiency parameter and form factor arising from measurement noise.[16]

The literature review illustrates that the challenge of estimation accuracy for engine cylinder pressure arises from the parametric uncertainties. Hence, motivated by the V2V in T-CPS context, this study seeks to reduce the influence of parametric uncertainties on the estimation accuracy for effective engine cylinder pressure. Specifically, a high gain observer based on the engine dynamic model is designed with the consideration of its inherent robustness properties, as well as the ability to reject model uncertainties.[25–30] Then, the analyses of convergence, converge speed and stability of the corresponding error model are performed using the Laplace and Lyapunov method. Finally, numerical experiments are carried out to demonstrate the effectiveness of the proposed approach.

The rest of the paper is organized as follows. Section 2 designs the high gain observer based on the engine dynamic model and conducts the analyses of convergence, converge speed, and stability of the corresponding error model. Section 3 performs the simulink-based numerical experiments and compares the performance of the proposed method with those of the second-order SMO and the traditional SMO. The final section concludes this study.

2. High-gain observer design

2.1. Engine dynamic model

Based on Refs. [16] and [17], a single zone thermodynamics combustion model is used to describe the dynamics of cylinder pressure, where the in-cylinder charge is assumed to be homogeneous and the pressure, temperature, and cylinder charge are uniform within the cylinder. Then, the engine pressure dynamics equation can be written as follows:[16]

$$\dot{p} = \frac{\gamma - 1}{V}\left(\dot{Q}_{\text{ch}} - \dot{Q}_{\text{ht}}\right) - \frac{\gamma}{V}\dot{V}p, \tag{1}$$

where p, γ, $\dot{Q}_{\text{ch}}$, and V are represented by the cylinder pressure (Pa), the polytropic coefficient, the combustion heat release rate (kW), and total cylinder volume (m³), respectively, and $\dot{Q}_{\text{ht}}$ is the heat transfer rate which can be treated as part of $\dot{Q}_{\text{ch}}$, i.e., $\dot{Q}_{\text{ht}} = \alpha\dot{Q}_{\text{ch}}$, α is the heat loss coefficient, which is generally gathered near 0.82.[14]

The term $\dot{Q}_{\text{ch}}$ can be expressed in terms of the lower heating value Q_{LHV} (kJ/kg) and the burning rate of the fuel $\dot{m}_{\text{b}}$ (kg/s), i.e.,[16,17]

$$\dot{Q}_{\text{ch}} = m_{\text{f}}\dot{m}_{\text{b}}Q_{\text{LHV}}, \tag{2}$$

where Q_{LHV} can be obtained in fuel table, m_{f} (kg) is the injected fuel mass, and

$$m_{\text{b}} = 1 - \exp\left(-a\left(\frac{\theta - \theta_0}{\Delta\theta}\right)^{m+1}\right), \tag{3}$$

where a and m represent the efficiency parameter and the form factor, respectively, θ, θ_0, and $\Delta\theta$ are crank angle (°), initial angle of combustion (°), and the total angle during the combustion duration (°).

Moreover, the total cylinder volume V in Eq. (1) consists of the combustion chamber volume V_{c} and the cylinder work volume V_{s}, i.e.,[16,17]

$$V = V_{\text{s}} + V_{\text{c}}, \tag{4}$$

where $V_{\text{c}} = \pi D^2 S/(4(r-1))$, $V_{\text{s}} = A_{\text{p}}y_{\text{p}}$, and r, D, S, and A_{p} are the compression ratio, the cylinder diameter (m), the displacement of piston (m) and the piston cross-sectional area (m²), respectively, and y_{p} is the piston position (m), which is given by[16,17]

$$\begin{cases} y_{\text{p}} = L + R - (R\cos\theta + \sqrt{L^2 - (R\sin\theta)^2}), \\ A_{\text{p}} = \dfrac{\pi D^2}{4}, \end{cases} \tag{5}$$

where L and R represent the length of connecting rod (m) and the crank radius (m), respectively. Therefore, the cylinder volume rate can be written as

$$\dot{V} = \dot{V}_{\text{s}} + \dot{V}_{\text{c}} = A_{\text{p}}\dot{y}_{\text{p}}. \tag{6}$$

2.2. Observer design

In order to design the observer, the state of engine cylinder pressure can be defined as

$$\boldsymbol{x} = [\,x_1\ x_2\,]^{\text{T}} = [\,p\ \dot{p}\,]^{\text{T}}. \tag{7}$$

Then, the state-space representation of Eq. (1) can be obtained[31]

$$\begin{cases} \dot{x}_1 = x_2 = \varphi_1(x,u), \\ \dot{x}_2 = \dfrac{\gamma^2}{V^2}\dot{V}^2 x_1 - \dfrac{\gamma(\gamma-1)\dot{V}}{V^2}(1-\alpha)\dot{Q}_{\text{ch}} = \varphi_2(x,u), \end{cases} \tag{8}$$

where $\varphi_2(x,u)$ satisfies the Lipschitz condition, i.e., $\|\varphi_2(x,u) - \varphi_2(\hat{x},u)\| \le \lambda\,\|x - \hat{x}\|$, and $\lambda > 0$ is the Lipschitz constants. Under steady-state conditions, the engine states and parameters are nonzero, so the Jacobi matrix of Eq. (8) is as follows:

$$\boldsymbol{J} = \begin{bmatrix} \dfrac{\partial\varphi_1}{\partial x_1} & \dfrac{\partial\varphi_1}{\partial x_2} \\ \dfrac{\partial\varphi_2}{\partial x_1} & \dfrac{\partial\varphi_2}{\partial x_2} \end{bmatrix} = \begin{bmatrix} 0 & 1 \\ \left(\dfrac{\gamma}{V}\dot{V}\right)^2 & 0 \end{bmatrix}, \tag{9}$$

when the piston moves to top dead center (TDC) and bottom dead center (BDC), $\dot{V} = 0$, which means $r(\boldsymbol{J}) = 1$. Analysis has found that the cylinder pressure is observable at any position besides TDC and BDC where $r(\boldsymbol{J}) = 1$.[26]

According to Eq. (8), a high gain observer is proposed for cylinder pressure estimation, i.e.,

$$
\begin{cases}
\dot{\hat{x}}_1 = \hat{x}_2 + h_1(x_1 - \hat{x}_1), \\
\dot{\hat{x}}_2 = \varphi_2(\hat{x}, u) + h_2(x_1 - \hat{x}_1),
\end{cases}
\tag{10}
$$

where $\hat{\boldsymbol{x}} = [\hat{x}_1 \ \hat{x}_2]^{\mathrm{T}}$ represents the observer states and the observer gains h_1 and h_2 are designed in the following analysis to ensure that the state error is small as desired. The state error is defined as the error between the actual state and the estimation state, i.e., $\tilde{x} = x - \hat{x}$. Then, the error model is given based on Eqs. (8) and (10)

$$
\begin{cases}
\dot{\tilde{x}}_1 = \tilde{x}_2 - h_1\tilde{x}_1, \\
\dot{\tilde{x}}_2 = \delta(\tilde{x}, u) - h_2\tilde{x}_1,
\end{cases}
\tag{11}
$$

where $\delta(\tilde{x}, u) = \varphi_2(x, u) - \varphi_2(\hat{x}, u)$.

2.3. Convergence analysis

For the designed observer (see Eq. (10)), the convergence of estimation errors should be guaranteed, which motivates us to conduct the Laplace transformation of the error model (11) and check whether it is robust to the parametric uncertainties arising from the measurement noise. Based on Eqs. (10) and (11), two kinds of situations are considered as follows.

On the one hand, the error model (11) is addressed under the assumption that the engine dynamic model (1) is a precise description of the object, that is to say, $\delta(\cdot)$ is not considered in Eq. (11), and we obtain

$$
\dot{\tilde{x}} = A_0\tilde{x},
\tag{12}
$$

where $A_0 = \begin{bmatrix} -h_1 & 1 \\ -h_2 & 0 \end{bmatrix}$.

Based on Eq. (12), the observer states $\hat{\boldsymbol{x}} = [\hat{x}_1 \ \hat{x}_2]^{\mathrm{T}}$ will approach to the state $\boldsymbol{x} = [x_1 \ x_2]^{\mathrm{T}}$ in finite time if A_0 is a Hurwitz matrix. Therefore, the gain $\boldsymbol{h} = [h_1 \ h_2]^{\mathrm{T}}$ needs to ensure that A_0 is a Hurwitz matrix, which means the eigenvalues of A_0 are negative.

On the other hand, it is necessary to take the influence of $\delta(\cdot)$ to $\tilde{x}$ into consideration since the fluctuation of the parameters a and m will lead to inevitable errors. Therefore, considering the presence of $\delta(\cdot)$, we have

$$
\begin{cases}
s\tilde{x}_1 = -h_1\tilde{x}_1 + \tilde{x}_2, \\
s\tilde{x}_2 = -h_2\tilde{x}_1 + \delta,
\end{cases}
\tag{13}
$$

that is

$$
\begin{cases}
\tilde{x}_2 = \tilde{x}_1(s + h_1), \\
s^2\tilde{x}_1 = -h_1 s\tilde{x}_1 + \tilde{x}_2 s = -h_1 s\tilde{x}_1 - h_2\tilde{x}_1 + \delta.
\end{cases}
\tag{14}
$$

The transfer function of Eq. (14) is

$$
\begin{cases}
G_{10}(s) = \dfrac{\tilde{x}_1(s)}{\delta(s)} = \dfrac{1}{s^2 + h_1 s + h_2}, \\
G_{20}(s) = \dfrac{\tilde{x}_2(s)}{\delta(s)} = \dfrac{\tilde{x}_1(s)}{\delta(s)}(s + h_1) = \dfrac{s + h_1}{s^2 + h_1 s + h_2}.
\end{cases}
\tag{15}
$$

In terms of $G_{10}(s)$, we obtain

$$
\begin{aligned}
A(G_{10}(\mathrm{j}\omega)) &= \left| \frac{1}{-\omega^2 + h_1\mathrm{j}\omega + h_2} \right| \\
&= \frac{1}{\sqrt{(h_2 - \omega^2)^2 + h_1^2\omega^2}}.
\end{aligned}
\tag{16}
$$

If h_1 and h_2 are large enough, i.e., $h_1 \gg 1$, $h_2 \gg 1$, then $A(G_{10}(\mathrm{j}\omega)) \to 0$ and $\tilde{x}_1 \to 0$ can hold.

Similarly, according to $G_{20}(s)$, we have

$$
\begin{aligned}
A(G_{20}(\mathrm{j}\omega)) &= \left| \frac{h_1 + \mathrm{j}\omega}{-\omega^2 + h_1\mathrm{j}\omega + h_2} \right| \\
&= \sqrt{\frac{h_1^2 + \omega^2}{(h_2 - \omega^2)^2 + h_1^2\omega^2}}.
\end{aligned}
\tag{17}
$$

If $h_2 \gg h_1$, then $A(G_{20}(\mathrm{j}\omega)) \to 0$ and $\tilde{x}_2 \to 0$ is also guaranteed.

Based on the foregoing discussion, considering the combination of the condition $h_1 \gg 1$, $h_2 \gg 1$ with the condition $h_2 \gg h_1$, if $h_2 \gg h_1 \gg 1$, we will have $\tilde{\boldsymbol{x}} = [\tilde{x}_1 \ \tilde{x}_2]^{\mathrm{T}} \to 0$, which validates the convergence of the error model (11).

Furthermore, the transfer function of Eq. (15) can be rewritten as

$$
G_0(s) = \begin{bmatrix} G_{10}(s) \\ G_{20}(s) \end{bmatrix} = \frac{\tilde{x}}{\delta} = \frac{1}{s^2 + h_1 s + h_2}\begin{bmatrix} 1 \\ s + h_1 \end{bmatrix}.
\tag{18}
$$

Let

$$
h_1 = \frac{\alpha_1}{\varepsilon}, \quad h_2 = \frac{\alpha_2}{\varepsilon^2},
\tag{19}
$$

where $\alpha_1, \alpha_2 \in \mathbb{R}$, and $\alpha_1, \alpha_2 > 0$, and $0 < \varepsilon \le 1$ which implies $h_2 \gg h_1 \gg 1$.

By substituting Eq. (19) into Eq. (18), we can obtain

$$
\begin{aligned}
G_0(s) &= \frac{1}{s^2 + \dfrac{\alpha_1}{\varepsilon}s + \dfrac{\alpha_2}{\varepsilon^2}}\begin{bmatrix} 1 \\ s + \dfrac{\alpha_1}{\varepsilon} \end{bmatrix} \\
&= \frac{\varepsilon}{(\varepsilon s)^2 + \alpha_1\varepsilon s + \alpha_2}\begin{bmatrix} \varepsilon \\ \varepsilon s + \alpha_1 \end{bmatrix}.
\end{aligned}
\tag{20}
$$

Hence, we know that $G_0(s) \to 0$ if $\varepsilon \to 0$. This means that the designed observer is robust to the parametric uncertainties arising from the measurement noise.

Remark 1 According to Eqs. (18)–(20), we can draw a conclusion that error model of the proposed observer is convergent towards zero if the gain parameters are designed reasonably, especially when the condition $h_2 \gg h_1 \gg 1$ is satisfied. Therefore, the rejection of parametric uncertainties can be achieved. In other words, the proposed observer is robust to parametric uncertainties.

2.4. Convergent speed analysis

Actually, the error model (11) can be rewritten as

$$\dot{\tilde{x}} = A_1 \tilde{x}, \tag{21}$$

where

$$A_1 = \begin{bmatrix} -h_1 & 1 \\ \left(\dfrac{\gamma}{V}\dot{V}\right)^2 - h_2 & 0 \end{bmatrix}.$$

The solution of Eq. (21) is

$$\tilde{x}(t) = \mathrm{e}^{A_1 t} e(0). \tag{22}$$

Hence

$$\|\tilde{x}(t)\| = \left\| \mathrm{e}^{A_1 t} e(0) \right\|. \tag{23}$$

According to the convergence analysis, we know that A_1 is stable. So $\exists \, \rho, \varsigma > 0$ and $\rho, \varsigma \in \mathbb{R}$, s.t. $\left\| \mathrm{e}^{A_1 t} \right\| \leq \rho \, \mathrm{e}^{-\varsigma t}$ which implies if $t \to \infty$, then $\left\| \mathrm{e}^{A_1 t} e(0) \right\| \to 0$. Note that the convergence time is determined by A_1. Thus we can adjust the gains h_1 and h_2 to change the convergent speed.

2.5. Stability analysis

According to the errors model (11), we choose the Lyapunov function candidate as

$$E = \frac{1}{2}\tilde{x}_1^2 + \frac{1}{2}\tilde{x}_2^2. \tag{24}$$

Taking the time derivative of the Lyapunov function gives

$$\dot{E} = \tilde{x}_1 \dot{\tilde{x}}_1 + \tilde{x}_2 \dot{\tilde{x}}_2. \tag{25}$$

Based on Eq. (11), the following equation is derived:

$$\begin{aligned} \dot{E} &= \tilde{x}_1 \tilde{x}_2 - h_1 \tilde{x}_1^2 + \delta \tilde{x}_2 - h_2 \tilde{x}_1 \tilde{x}_2 \\ &= \left[\left(\frac{\gamma}{V}\dot{V}\right)^2 + 1 - h_2 \right] \tilde{x}_1 \tilde{x}_2 - h_1 \tilde{x}_1^2. \end{aligned} \tag{26}$$

In terms of Eq. (26), $\dot{E} < 0$ if $h_1 > 0$ and $h_2 = (\gamma \dot{V}/V)^2 + 1$ are satisfied. Hence, the designed gains h_1 and h_2 can stabilize the proposed observer (10) based on the Lyapunove theory.

Remark 2 Based on Eqs. (24)–(26), it can be seen that the stability of the proposed observer depends on the gains h_1 and h_2. If h_1 and h_2 are designed reasonably, the stability is guaranteed, and which also means the designed observer can estimate the state variables steadily.

Remark 3 The analyses of Sections 2.3–2.5 are conducted based on the observer error model (11). Section 2.3, which focuses on convergence, validates that the proposed observer (10) can reject the parametric uncertainties, which means the observer (10) is robust. Section 2.4, which focuses on the convergent speed, verifies that the convergent speed can be adjusted by changing the gains h_1 and h_2. Section 2.5, which focuses on stability, indicates that the proposed observer (10) can estimate the cylinder pressure with stability, which also infers that the designed observer (10) is stable.

3. Numerical experiments

In order to demonstrate the performance of the proposed high gain observer, we perform the simulations with an engine speed of 3600 (r/min). The specific steps are as follows.

Step 1 Build the cylinder engine model using GT-Power, and let the engine work under a large and small load;

Step 2 Incorporate Matlab/Simulink platform with the cylinder pressure model and the high gain observer based on Eqs. (1), (8), (10), and so on;

Step 3 Combine GT-Power with Simulink; and,

Step 4 Test gains h_1 and h_2 in selected ranges and find the reasonable values to make the errors stable and small.

The parameters associated with the engine are set as: $\gamma = 1.085$, $\theta_0 = -20°$, $\Delta\theta = 40°$. The whole Simulink main program is shown in Fig. 1 and the engine specifications are listed in Table 1.

The engine cylinder pressure is estimated from compression stroke to exhaust stroke and the estimation error is defined as $e = |(\hat{p} - p)/p| \times 100\%$. Firstly, the simulation is carried out under small (with the throttle opening angle $5°$) and large load (with the throttle opening angle $75°$) conditions with the gain parameters h_1 and h_2 based on Eqs. (19) and (26), and with parameters $a = 5$, $m = 3$, respectively. The results are shown in Figs. 2–4.
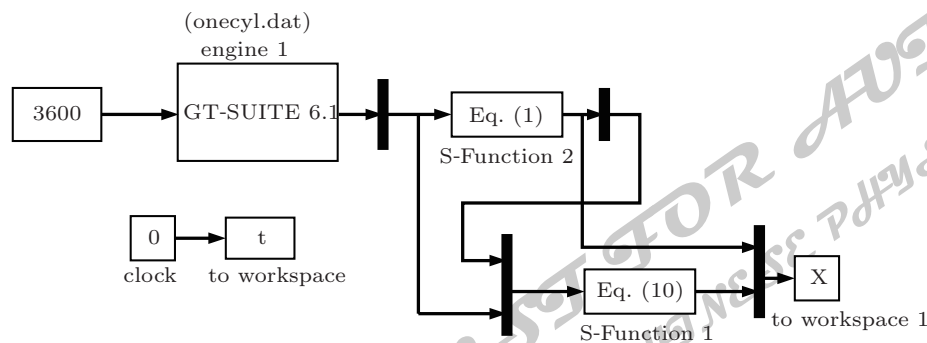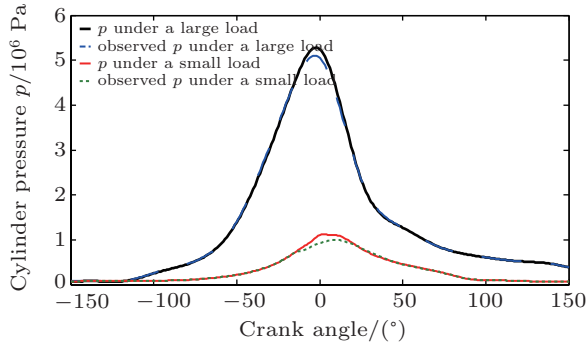

Fig. 1. Simulink main program.

Table 1. Engine specifications.

Basic parameter	Specific configuration
Intake type	natural aspiration
Number of cylinders	1
Cylinder diameter D/m	0.1
Displacement of piston S/m	0.1
Length of connecting rod L/m	0.22
Crank radius R/m	0.05
Capacity/L	0.876

Fig. 2. (color online) Observed cylinder pressure and simulated "actual" pressure under large and small loads.

From Fig. 2 it can be seen that the cylinder pressures estimated by the proposed observer generally approximate to the simulated "actual" pressure under large and small loads, respectively. In addition, from Fig. 3, we know that estimation errors start to increase before the piston approaches close to TDC and to decrease when the piston takes away from the TDC. This happens because the system states are unobservable at TDC. However, the proposed high gain observer can also keep the estimation error under about 20%.
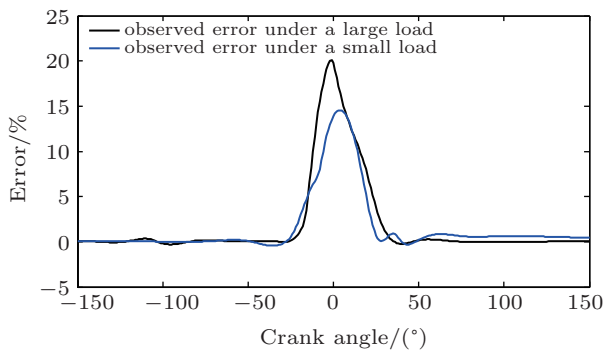
Fig. 3. (color online) Estimation error under large and small loads.

On the other hand, the comparisons of accuracy around the TDC with the second-order SMO in Ref. [17] and the traditional SMO in Ref. [24] are conducted, and the corresponding observation errors are listed in Table 2.

As shown in Table 2, comparatively speaking, the errors for high pressure and low pressure in Refs. [17] and [24] are larger than that in the proposed high gain observer around the TDC region. To account for this phenomenon, a reasonable

explanation may be that the second-order SMO in Ref. [17] is unobservable around the TDC region, which results in the pressure error determined mainly by the model error; while the chattering of the observer and the parameters errors in the traditional SMO in Ref. [24] may lead to the error increase. In other words, it shows that the proposed high gain observer has a better ability to avoid the uncertainties from the model. Therefore, the accuracy of the cylinder pressure estimation in proposed high gain observer is guaranteed, even around the TDC regions.

Table 2. Error comparison.

Method	Error under a large load	Error under a small load
Second-order SMO in Ref. [17]	< 30%	< 20%
Traditional SMO in Ref. [24]	< 40%	< 50%
High gain observer	< 14.6%	< 19.8%

Furthermore, in order to verify the robustness to parametric uncertainties, another simulation is carried out with parameters $a = 3$, $m = 2$, and the result is shown in Fig. 4. Figure 4 shows that the accuracy of the designed observer is higher (about 19.8%) than that of the traditional SMO in Ref. [24] (about 30%) even the parameters are changed. That is to say, the robustness of the high gain observer is better than that in Ref. [24].
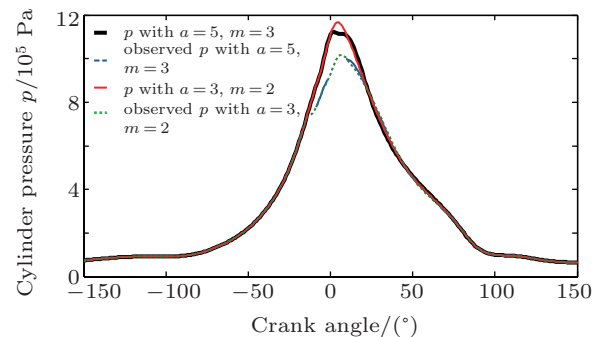
Fig. 4. (color online) Observed cylinder pressure and simulated actual pressure under a small load with different parameter values.

According to the above discussion, we can draw a conclusion that the proposed high gain observer can not only reject the parametric uncertainties but also has a better robustness and higher accuracy of the cylinder pressure estimation.

4. Conclusion

To ensure the reliability and accuracy of the cylinder pressure within information exchange under the V2V communications in T-CPS, a high gain observer is designed to reject the parametric uncertainties and improve the estimation accuracy. After the theoretical analyses about convergence, converge speed and stability of the corresponding error model, the proposed observer is proved to be robust and stable and

the convergent speed can be adjusted with the gains h_1 and h_2. Finally, numerical experiments and comparisons with the second-order SMO and the traditional SMO are performed. The results verify the effectiveness of the proposed approach with respect to robustness and accuracy.

References

[1] Li Y, Zhu H, Li P, Cen M, Li Y G and Sun D 2013 *Proceedings of the* 2*nd International Conference on Transportation Information and Safety*, June 29–July 2, 2013, Wuhan, China, p. 64

[2] Sun D, Li Y, Liu W, Zhao M and Liao X 2013 *Chin. J. Highway Transport* **26** 144

[3] Yao J, Huang J Y, Chen G R and Xu W S 2013 *Acta Phys. Sin.* **22** 060208 (in Chinese)

[4] Qian Y, Shi P and Zeng Q 2009 *Chin. Phys. B* **18** 4037

[5] Xie D, Gao Z and Zhao X Z 2008 *Chin. Phys. B* **17** 4440

[6] Xiao Y and Zheng J F 2013 *Acta Phys. Sin.* **62** 178902 (in Chinese)

[7] Li L, Wen D and Yao D 2014 *IEEE Trans. Intell. Transp. Syst.* **15** 425

[8] Tang T, Shi W, Shang H and Wang Y 2014 *Nonlinear Dyn.* **76** 2017

[9] Tang T, Shi W, Shang H and Wang Y 2014 *Measurement* **58** 286

[10] Jin W and Recker W 2006 *Transportation Research Part B: Methodological* **40** 230

[11] Jin W and Recker W 2010 *IEEE Trans. Wirel. Commun.* **9** 106

[12] Shu G, Pan J and Wei H 2013 *Appl. Therm. Eng.* **51** 1297

[13] Yu S, Choi H and Cho S 2013 *Int. J. Auto. Technol.* **14** 175

[14] Hurnheer T and Soltic P 2012 *Control Eng. Practice* **20** 293

[15] Yoon M, Lee K and Sunwoo M 2007 *Mechatronics* **17** 469

[16] Aldurra A A, Fiorentini L and Canova M 2011 *American Control Conference*, June 29–July 1, 2011, San Francisco, California, USA, p. 991

[17] Wang Y, Chun F and Guo D 2004 *Trans. CSICE* **22** 555

[18] Durra A A, Canova M and Yurkovich S 2009 *Proceedings of the ASME Dynamic Systems and Control Division*, 2009, America, p. 175

[19] Ozawa A and Sanada K 2011 *SICE Annual Conference*, September 13–15, 2011, Tokyo, Japan, p. 1457

[20] Moro D, Cavina N and Ponti F 2002 *J. Eng. Gas. Turbines Power-Trans. ASME* **124** 220

[21] Hamedovic H, Raichle F and Breuninger J F 2005 *IEEE International Conference on Acoustics, Speech and Signal Processing*, March 19–25, 2005, Philadelphia, USA, p. 677

[22] Yuan L, Shen J Q, Xiao F and Chen M L 2013 *Acta Phys. Sin.* **62** 030501 (in Chinese)

[23] Veluvolu K C and Soh Y C 2007 *Proceedings of the* 46*th IEEE Conference on Decision and Control*, December 12–14, 2007, New Orleans, LA, USA, p. 4348

[24] Shiao Y and Moskwa J 1995 *IEEE Trans. Control Syst. Technol.* **3** 70

[25] Khalil H and Praly L 2014 *Int. J. Robust Nonlinear Control* **24** 993

[26] Dai X, Gao Z, Breikin T and Wang H 2012 *IEEE Trans. Auto. Control* **57** 726

[27] Jiang L, Wu Q H and Wen J Y 2004 *IEEE Trans. Circ. Syst.* **51** 2052

[28] Li Y, Ren C and Tong S 2012 *Nonlinear Dyn.* **67** 1175

[29] Ahrens J H and Khalil H K 2009 *Automatica* **45** 936

[30] Han D and A Zhu F L 2013 *Acta Phys. Sin.* **62** 120513 (in Chinese)

[31] Ahmed Q and Bhatti A 2011 *IEEE Trans. Ind. Electron.* **58** 4837